Applied Surface Science 467–468 (2019) 749–752

Contents lists available at ScienceDirect

Applied Surface Science

journal homepage: www.elsevier.com/locate/apsusc

Short Communication

Monitoring the energy of the metal ion-content plasma-assisted deposition and its implication for bacterial inactivation

Sami Rtimi[a,b,*], Victor Nadtochenko[c], Inessa Khmel[d], Stéphanos Konstantinidis[e], Nikolay Britun[e], John Kiwi[a,*]

[a] Ecole Polytechnique Fédérale de Lausanne, EPFL-SB-ISIC-GPAO, Station 6, CH-1015 Lausanne, Switzerland
[b] Ecole Polytechnique Fédérale de Lausanne, EPFL-STI-LTP, Station 12, CH-1015 Lausanne, Switzerland
[c] N.N.Semenov Institute of Chemical Physics RAS, Kosigin str.4, Moscow 119991, Russia
[d] Institute of Molecular Genetics, Russian Academy of Sciences, Kurchatov sq.2, 123182 Moscow, Russia
[e] Chimie des Interactions Plasma-Surface, Université de Mons, Place du parc 23, 7000 Mons, Belgium

ARTICLE INFO

Keywords:
Cu-polyester
Magnetron sputtering
Cu-ions
Porinless bacteria
Bacterial inactivation
Surface-contact effect

ABSTRACT

Cu-polyester (Cu-PES) was sputtered by high power impulse magnetron sputtering (HIPIMS) and by low energy direct current magnetron sputtering (DCMS). The total amount and distribution of the Ar^+, Cu^+ and Cu^{2+} ions were determined as well as the bacterial inactivation kinetics mediated by DCMS and HIPIMS samples. The separation of extracellular and intracellular processes leading to bacterial inactivation was assessed on normal and genetically modified *E. coli*.

1. Introduction

Cu has been increasingly investigated during the last decade due to its higher cytotoxicity compared to Ag. The interest is in the preparation of more advanced Cu-based materials leading to an accelerated bacterial inactivation kinetics. Cu-surfaces showing increased adhesion, longer operational lifetimes and faster bacterial instantaneous kinetics are therefore addressed in this study. Cu-surfaces containing highly dispersed Cu-nanoparticles (Cu-NPs) and leading to bacterial inactivation have been recently reported by Borkow [1], Espirito-Santo [2], Amal [3], Gedanken [4], Pillai [5], Dionysiou [6], and Trampuz [7]. In addition, the use of Cu-NPs in implants/catheters is in the increase and can be found in new products hitting the market as reported by Bader [8] and Vasilev [9]. The Cu-cytotoxicity per unit weight [10] is higher compared to the cytotoxicity reported by Ag, Pd and Zn-ions [11] leading favourably to bacterial inactivation. Cu-colloidal Cu-suspensions on diverse thermal resistant substrates have been reported but the polymers (such as polyester, PES) does not allow the annealing of Cu at a few hundred degrees. When Cu-colloids are impregnated on textiles and heated to lower temperatures to induce adhesion the coating obtained is not uniform nor adhesive [12]. By physical vapour deposition (PVD), Cu-films have been depositing on substrates not needing any annealing. Contrarily, Chemical Vapour Deposition (CVD) requires high temperature and demands a costly cooling system [13]. Low temperature Cu-deposition of uniform, robust and adhesive Cu/Cu_2O/CuO films is possible by DCMS [14] and HIPIMS [15] at temperatures of 110–130 °C. These temperatures are within the thermal limit of textiles and some other polymers. HIPIMS induced up to 70% Cu-ionization leading concomitantly to more compact and less corrosive Cu-films compared to DCMS [15].

Natural *E. coli* K12 bacteria of one micron in size present porin channels of 1.1–1.3 nm [17] regulating the diffusion/flow of the metabolic important Na, K, Fe, Ca and Mg-ions in and out of the cell [18]. The effect of the Cu-surface regulating the Cu-ions leading cell inactivation/*lysis*/death was sorted out employing genetically modified porinless *E. coli*. The latter porinless *E. coli* mutant strain deficient in OmpF or OmpC genes was prepared according to the protocols cited in references [19,20]. The porinless *E. coli* bacterial cell envelope is not able to transfer ions to the cytoplasm but gets damaged by contact with the Cu-PES samples. The natural *E. coli K12* ATCC is isogenic with the genetically modified *E. coli* porinless bacteria. The *E. coli* K12 and the *E. coli* TK 821 were analysed at the same growth phase to limit possible concentration changes during the bacterial inactivation. The OD was monitored at 600 nm until it reached the exponential growth phase of ~OD 0.6. The OD-values for both stains were similar. This is indicative that the genetic differences between these two strains do not influence

* Corresponding authors at: Ecole Polytechnique Fédérale de Lausanne, EPFL-STI-LTP, Station 12, CH-1015 Lausanne, Switzerland (S. Rtimi and J. Kiwi).
E-mail addresses: sami.rtimi@epfl.ch (S. Rtimi), john.kiwi@epfl.ch (J. Kiwi).

https://doi.org/10.1016/j.apsusc.2018.10.207
Received 24 May 2018; Received in revised form 14 September 2018; Accepted 25 October 2018
Available online 28 October 2018
0169-4332/

the cell growth.

This study addresses: (a) the amount and ionic distribution of Cu-species sputtered by DCMS and HIPIMS, (b) the effect of the samples sputtered with different plasma energies on the bacterial inactivation kinetics and finally, (c) the gene mutation effect of the encoding OmpF and OmpC porins on the *E. coli* bacterial inactivation kinetics providing the evidence for the surface-contact effects leading to bacterial inactivation (without ions diffusion).

2. Experimental

Copper films were sputtered on PES by DCMS or by HIPIMS. HIPIMS was carried out applying a pulsed voltage, repetition frequency and duration adapted to control the time-averaged power delivered to the plasma. HIPIMS was carried out at a time-averaged power of 100 +/ −10 W. The pulse duration during the sputtering were in the range of 10–50 μs, the target voltage from 500 to 900 V and target currents of 20, 40, 80, and 100A. A Cu-target 5 cm in diameter was used in the magnetron chamber at a base pressure $< \sim 5 \times 10^{-6}$ Torr. The PES-samples were set 6 cm above the Cu-target. The Cu-atoms sputtered on the PES presented an energy of 10 eV in Ar ionized at 500 V. The Cu-distribution followed a first order cosine pattern perpendicular to the PES-surface. About 30% of the Cu-ions/atoms were emitted at an angle of 30 degrees. When pressures < 1 Pascal were used, the ionized Cu-atoms undergo almost no collisions, conserving most of their initial kinetic energy and penetrate the PES up to one or two atomic layers. The total amount of ions and the ion-energies were monitored mass spectrometry using a Hiden HAL7-EQP1000 mass-energy analyser. The floating potential was aligned with the analyzer PES-potential. The ion-energy distribution function (IEDF) allowed to determine the relative ion fractions of Ar^+, Cu^+ and Cu^{2+}-ions as shown in Figs. 1a/1b

An overnight culture of *E. coli* (usually 2–5 × 10^9 cells/ml) grown in a Laura Bertani (LB) solution is diluted 1000-fold in saline solution (0.85% NaCl in distilled water). The bacteria were incubated in the dark under aerobic conditions until reaching an exponential growth phase of 0.6. The 1% dilution was then transferred into a fresh LB-solution and the bacterial incubation extended up to 15 h. The samples of Cu-PES in contact with bacteria were irradiated inside a cavity by way of an Osram Lumilux 18 W/827 actinic light source (360–700 nm, 4.5 mW/cm^2; see supplementary Fig. S1). At pre-selected times, the inoculated Cu-PES sample was washed with saline solution and the cell suspension collected into an Eppendorf tube. A 100 μl bacterial suspension were seeded on Petri dish containing plate count agar. This proceeding follows the bacterial evaluation according to a protocol used during the last few years [11,16,23,27].

Supplementary data associated with this article can be found, in the online version, at https://doi.org/10.1016/j.apsusc.2018.10.207.

Scanning transmission electron microscopy (STEM) was carried out in an FEI Osiris instrument operated at 200 kV with spot size of 5, dwell time 50 and real time 600 s for the Cu-PES samples. Further details of the STEM technique used have been recently reported [21]. The film X-ray photoelectron spectroscopy (XPS) was carried out using an AXIS NOVA photoelectron spectrometer (Kratos Analytical, Manchester, UK) provided for with a monochromatic (AlKαhν = 1486.6 eV) anode. The surface atomic percentage concentration was determined from the peak areas using the known sensitivity factors for each element [22]. The Cu-content of the Cu-PES samples was determined by X-ray fluorescence (XRF) in a PANalytical PW2400 spectrometer and revealed a Cu-content for the DCMS (0.3 A) sample of 0.07% wt_{Cu}/wt_{PES}. The HIPIMS (20 A) sputtered sample presented a 0.10 wt%Cu/wt PES. Other Cu-PES samples were sputtered at 40–80 A and attained a Cu-content of 0.05 wt % Cu/wt PES.

3. Results and discussions

Fig. 1a presents the results for the total number of Cu-ions produced in the magnetron chamber by DCMS and by HIPIMS-sputtering. The total number of Cu-ions and Ar-ions was the highest for the sample sputtered by HIPIMS at 20 A. This sample also presented the highest Cu-content as reported in the preceding paragraph. Fig. 1b shows the relative distribution of the three ionic-species. Fig. 1b shows that the HIPIMS (20 A) sample leading the highest amount of Ar^+-ions concomitantly presented the higher amounts of Cu^+-ions [14–16]. The excited Ar*-species with a higher energetic content relative to Cu, would ionize the Cu* as suggested in Eqs. (1) and (2). The Ar in the magnetron chamber under the applied current ionizes leading to Ar^+:

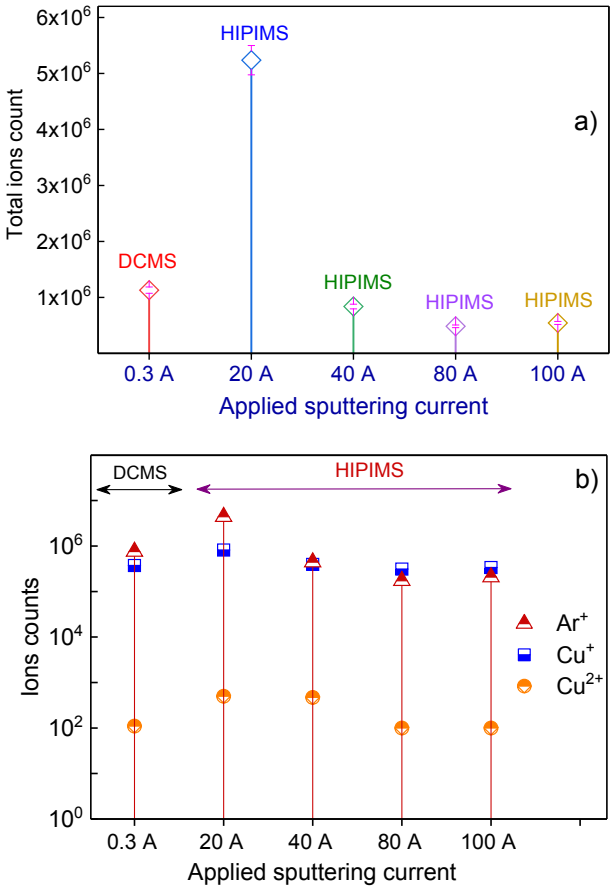

Fig. 1a. Total ions counting in plasma phase during the deposition of Cu on PES for 20 s as detected by a mass spectrometer coupled to the magnetron-sputtering unit. The DCMS sputtering was carried out at 0.3 A. HIPIMS-sputtering was carried out at different currents up to 100 A. Standard deviation of 10% for DCMS and 3% for HIPIMS deposition (Error bars: SD = 5%). (1b) Ion-species relative distribution in the plasma phase during the deposition of Cu on PES by DCMS and HIPIMS at different currents as monitored by the mass spectrometer coupled to the magnetron chamber.

$$Ar \rightarrow Ar^+ + e^- \text{ or } Ar^* + e^- \quad (1)$$

$$Ar^+ + CuO \rightarrow CuO^+ + Ar \quad (2)$$

$$e^- + CuO^0 \rightarrow CuO^+ + 2e^- \quad (3)$$

In Eq. (3), the high-energy electrons kick off an e^- of the Cu-target. The intensity of the e^- collision with the Cu^0 is proportional to the applied current. The Ar may also attain only excited states and ionize the CuO, as shown in Eq. (4), because the Ar has a higher energetic content than the ionization energy necessary to ionize CuO by a process called penning ionization:

$$Ar^* + CuO \rightarrow CuO^+ + Ar + e^- \quad (4)$$

Apparently, the Cu and Ar-ion collisions produced at lower densities

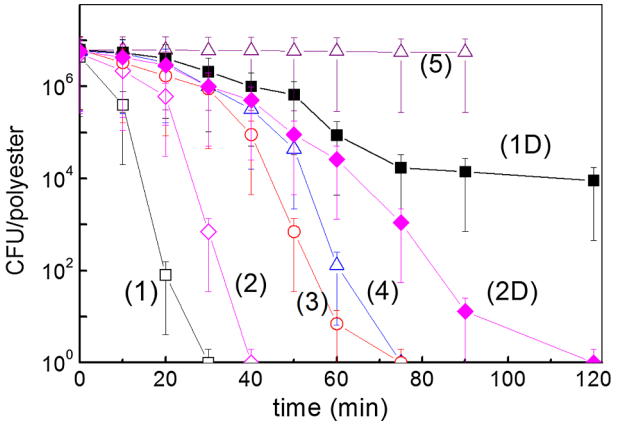

Fig. 2a. *E. coli* (K 12) light activated bacterial inactivation on Cu-PES sputtered at different energies for 20 s on Cu-PES samples: (1) HIPIMS at 20 A, (2) DCMS at 0.3 A, (3) HIPIMS at 40 A, (4) HIPIMS at 80 A, and (5) un-sputtered PES under indoor actinic light (4.5 mW/cm^2), (1D) HIPIMS at 20 A in the dark and (2D) DCMS at 0.3 A in the dark.

by HIPIMS 20 A are less intensive compared to the deactivation at higher ion-densities induced by higher currents and leads to a stronger deactivation of the ions in the plasma. This later point on top to the complexity of the ionization processes (Eqs. (1)–(4)) in the magnetron chamber may rationalize in part the data shown in Fig. 1a.

Fig. 2a shows that Cu-PES samples sputtered by HIPIMS (20 A) lead to the faster *E. coli* K12 inactivation. The control runs on un-sputtered PES and runs in the dark show that the Cu-PES sputtered with DCMS (0.3 A) led to a faster bacterial inactivation compared to HIPIMS (20 A) samples. Fig. 2a shows a slow initial stage leading to bacterial inactivation followed by a faster bacterial inactivation > 20–30 min. The bacterial inactivation kinetics induced by the HIPIMS sample was only a third faster compared to the DCMS-counterpart. Fig. 2a shows that the initial surface-contact between the Cu-PES and the bacteria requires some time (induction time) while introducing the damages leading to the increased cell permeability. Then, a faster second stage intracellular process sets in leading to bacterial inactivation. The monitoring of the bacterial inactivation as a function of time was carried out according to a method used for the last five years in our laboratory and extensively described above in the Experimental section in references [11,16,23,27].

The Cu-PES HIPIMS (20 A) sample induced *E. coli* inactivation within ~30 min as shown in Fig. 2a under low intensity actinic light irradiation. No release of Cu-ions after the 5th, 6th and 7th cycle was found as determined by ion-coupled plasma mass spectrometry (ICP-MS). A Finnigan^{TM} (ICP-MS) unit was used to follow the Cu-ion release during bacterial inactivation. The Cu-PES washing solutions were digested in nitric acid 69% (HNO_3:H_2O = 1:1), then the samples droplets were introduced into the ICP-MS at high temperatures. From the 1st and up to the 4th cycle a Cu-ion release was monitored < 6 ppb. These Cu-levels are below the limits allowed by the sanitary regulations for mammalian cells degradation [8,10,11,24].

The damage of the bacterial envelope in contact with the Cu-PES samples can be explained in terms of two different effects: a) the generation of reactive oxygen species (ROS) by Cu_xO-PES under actinic light and b) the destruction of the outer lipopolysaccharide (LPS) cell wall functional groups as followed by Fourier Transform Infrared Spectroscopy (FTIR) reported for Cu_xO in references [25–27]. In the magnetron chamber, a residual H_2O vapor equivalent to 10^{15} molecules/cm^{2}s or one H_2O-monolayer at Pr = 10^{-4} Pa remained. The monolayer decomposition produces enough O_2, atomic O and O-ions to oxidize the Cu-NPs to Cu_2O/CuO [28]. The generation of ROS-species leading to the damage/integrity of the outer bacterial cell in the reactions shown in Eqs. (5)–(10).

$$\text{Bacteria} + [Cu_xO\text{-PES}] + \text{light} \rightarrow [Cu_xO^*\text{-PES}]\ \text{Bacteria} \rightarrow \text{Bacteria}^+ + [Cu_xO\text{-PES}]\ cbe^- \quad (5)$$

$$[\text{Cu-PES}]vbh^+ + H_2O_{2ads} \rightarrow HO^0_{ads} + H^+ \quad (6)$$

$$[\text{Cu-PES}]cbe^- + O_2 + H^+ \rightarrow HO_2^{\cdot}\ E_0\text{-}0.05\text{NHE} \quad (7)$$

$$[\text{Cu-PES}]cbe^- + O_{2ads} \rightarrow O_{2ads}^{\cdot -}\ E_0\text{-}0.16\text{NHE} \quad (8)$$

$$[\text{Cu-PES}]vbh^+ + OH^-_{ads} \rightarrow HO^o \quad E_0\text{-}1.90\text{NHE} \quad (9)$$

$$HO_2^{\cdot} \Leftrightarrow O_2^{\cdot -} + H^+ pK_a 4.8 \quad (10)$$

The negative charge of the *E. coli* outer cell bilayers is due to the excess of carboxylic groups of the lipopolysaccharide (LPS) over the amide (I)/(II) groups [11,23] and interact with the Cu-PES positive surfaces at physiological pH-values between 6 and 8. During bacterial inactivation, the pH decreased by 1.2 pH-units (see Fig. 2) consistent with the reactions shown in Eqs. (6)–(10). The equilibrium at pH > 4.8 is displaced towards the right-hand side (see Eq. (10)) and implies an H^+-concentration increase > 10 times.

Fig. 2b presents the light induced inactivation kinetics for the genetically modified porinless *E. coli* TK821 compared to the *E. coli* K12 on the Cu-PES sputtered samples. Fig. 2b, traces 1 and 2 follow the bacterial inactivation trend reported in Fig. 2a. The Fig. 2b, traces 3 and 4 show a slower inactivation kinetics needing 60 min for the inactivation of the genetically modified *E. coli*. Fig. 2b, traces 3 and 4 shows the bacterial inactivation within 90 min on DCMS Cu-PES samples [28]. During disinfection, the reaction-pH decreased from 7.2 to 6.0 (see Fig. 2b).

Fenton-like Cu processes leading to reactive oxygen species (ROS) have been reported for Cu-ions [23]. Fig. 2b shows that for the porinless *E. coli*, the second stage intracellular process proceeds at a faster pace compared with the initial extracellular process taking place within ~20 min. The intracellular process sets in when Cu-ions are able to diffuse through the damaged cell envelope and reach the cell cytoplasm inducing cell death [1,13,18,23].

Binding and complexation between the positively charged Cu-PES samples and the negative cell envelope R-S-S-H, N- and COO^- functional groups lead to the bacterial degradation. The recycling of the HIPIMS Cu-PES (20 A) sample beyond the 4th cycle proceeded without the intervention of Cu-ions as determined by ICP-MS. This means that Cu-PES extracellular cytotoxicity may lead to bacterial inactivation in the absence of Cu-ions mainly responsible for the intracellular bacterial inactivation. This is a significant claim since the use of Cu/CuO/Cu-composites has been avoided until now to inactivate bacteria due to the

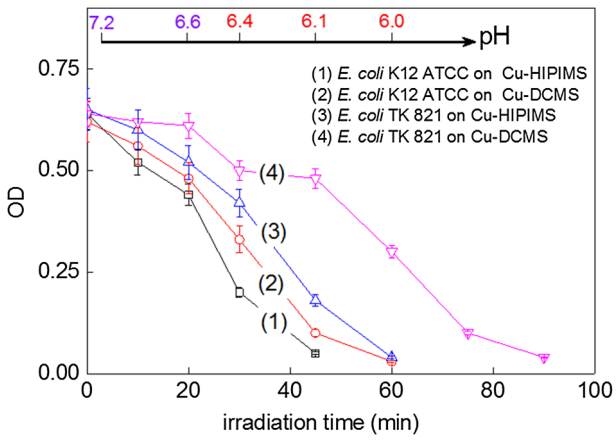

Fig. 2b. OD 600 optical density of *E. coli* K12 cells: normal porins *E. coli* (*omp*R$^+$ *omp*F$^+$*omp*C$^+$) versus porineless *E. coli* (*omp*R$^+$ *omp*F$^-$ *omp*C$^-$) on Cu-PES samples sputtered by HIPIMS (20 A). Runs on bacteria were carried out under low intensity actinic light irradiation (360 nm–700 nm; 4.5 mW/cm^2, SD: n = 5%) [28].

high Cu-ions cytotoxicity towards mammalian cells for treatment of wounds in the human body [10].

4. Conclusions

The first evidence is presented for the differentiated effect of the plasma energy used to deposit Cu on PES leading to distinct bacterial inactivation kinetics in natural *E. coli* and genetically modified porinless *E. coli*. The amounts of ions generated in the plasma phase (during the samples preparation/deposition) by DCMS and HIPIMS were identified by mass spectrometry. The main parameter controlling the bacterial inactivation kinetics was found to be the amount of Cu deposited on the Cu-PES surface. Genetically modified porinless bacteria were used to separate the effects of extracellular Cu-NPs and the intracellular Cu-ionic leading to bacterial inactivation. Cu-PES led to bacterial inactivation presenting a cytotoxicity below the levels allowed by the sanitary regulations for mammalian cells.

Acknowledgements

SR and JK thank EPFL, VN thanks the Russian Government support (0082-2018-0005 and AAAA-A18-118020690203) and SK is research associate of the Fund for Scientific Research (FNRS, Belgium).

References

[1] G. Borkow, J. Gabbay, Current. Chem. Bio. 3 (2000) 272–278.
[2] C. Espirito Santo, E. Lam, C. Elowsky, C. Quaranta, D. Domaille, C. Chang, G. Grass, Appl. Env. Microb. 77 (2011) 794–802.
[3] C. Gunawan, W. Teoh, C. Marquis, R. Amal, ACS Nano 5 (2011) 7214–7225.
[4] M. Eshed, J. Lellouche, S. Matalon, A. Gedanken, M. Banin, Langmuir 28 (2012) 1228–1234.
[5] M. Fisher, D. Keane, P. Fernandez-Ibanez, J. Colreavy, S. Hinder, K. McGuigan, S.C. Pillai, Appl. Cat. B: Environ. 130–131 (2013) 8–13.
[6] B. Banerjee, S.C. Pillai, P. Falaras, K. O'Shea, J.-A. Byrne, D. Dionysiou, J. Phys. Chem. Lett. 5 (2014) 2543–2554.
[7] L. Rio, E. Kusiak, J. Kiwi, C. Pulgarin, A. Trampuz, A. Bizzini, Appl. Environ. Microb. 78 (2012) 8176–8182.
[8] C. Zietz, A. Fritsche, B. Finke, V. Stranak, M. Haenle, R. Hippler, W. Mittelmeier, R. Bader, Bio-org. Chem. Appl. ID (2012) 850390.
[9] K. Vasilev, J. Cook, J. Griesser, Expert Rev. Med. Devices 6 (2000) 553–567.
[10] O. Bondarenko, K. Juganson, A. Ivask, K. Kasemets, M. Mortimer, A. Kahru, Crit. Rev. Arch. Toxicol. 87 (2013) 1118–1200.
[11] S. Rtimi, C. Pulgarin, R. Sanjines, J. Kiwi, Coatings 7 (2017) 20–49.
[12] L. Zhang, R. Dillert, D. Bahnemann, M. Vormoor, En. Environ. Sci. 5 (2012) 7491–7507.
[13] J-A Byrne, P.S.M. Dunlop, J.W. Hamilton, P. Fernandez-Ibanes, I. Polo-Lopez, P.K. Sharma, A.S.M. Vennard, Molecules 20 (2015) 5574–5612.
[14] K. Sarakinos, J. Alami, S. Konstantinidis, Surf. Coat. Technol. 204 (2010) 1661–1684.
[15] I. Petrov, A. Myers, J.E. Greene, J.R. Abelson, J. Vac. Sci. Technol. A 12 (1994) 2846–2851.
[16] S. Rtimi, O. Baghriche, C. Pulgarin, J.-C. Lavanchy, J. Kiwi, Surf. Coat. Technol. 232 (2013) 804–813.
[17] H. Nikaido, J. Biol. Chem. 269 (1994) 3905–3909.
[18] S. Robin, T. Soulimane, S. Lavelle, S.A.M. Tofail (Eds.), Biological Interactions with Surface Charges in Biomaterials, RSC London, UK, 2012.
[19] D. Sun, S.A. Crowell, C.M. Hardng, P.M. De Silva, A. Harrison, D.M. Fernando, K.M. Mason, E. Santana, P.C. Loewen, A. Kumar, Y. Liu, Life Sci. 148 (2016) 31–40.
[20] L.C. Seaver, J.A. Imlay, J. Bacter. 183 (2001) 7173–7181.
[21] S. Rtimi, R. Sanjines, C. Pulgarin, J. Kiwi, ACS Appl. Mater. Interf. 8 (2016) 56–63.
[22] C.D. Wagner, W.M. Riggs, L.E. Davis, J.F. Moulder, G.E. Mullenberg, Handbook of X-ray Photoelectron Spectroscopy, 2nd Ed, Minn, USA, 1979.
[23] S. Rtimi, V. Nadtochenko, I. Khmel, J. Kiwi, Chem. Comm. 53 (2017) 9093–9096.
[24] C. Zietz, A. Fritsche, B. Finke, V. Stranak, M. Haenle, R. Hippler, W. Mittelmeier, R. Bade, Bioorg. Chem. Appl. 2012 (2012) 850390.
[25] S. Rtimi, C. Pulgarin, M. Bensimon, J. Kiwi, Coll. Surf. B: Biointerf. 144 (2016) 222–228.
[26] S. Rtimi, C. Pulgarin, J. Kiwi, J. Adv. Oxid. Technols. 20 (2017) 1–8.
[27] S. Rtimi, C. Pillai, D. Dionysiou, J. Kiwi, Appl. Cat. B: Env. 240 (2019) 291–318.
[28] S. Rtimi, S. Konstantinidis, N. Britun, M. Bensimon, I. Khmel, V. Nadtochenko, App. Cat. B: Environ. 239 (2018) 245–253.